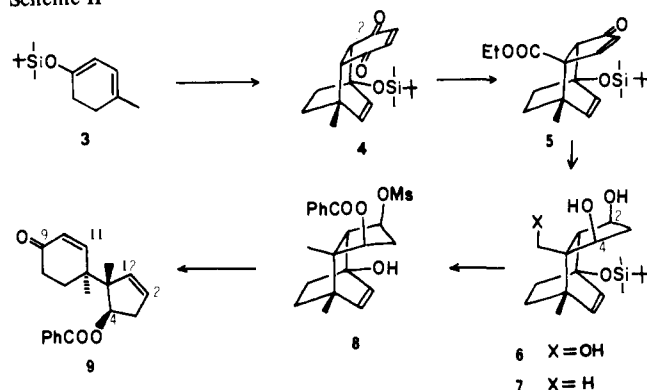
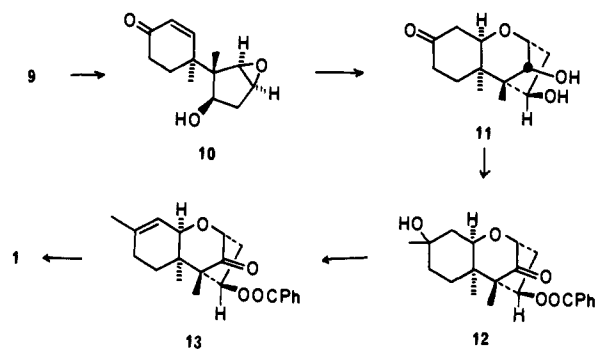


Scheme II



Scheme III



$C_5H_5N$ ; (2)  $Bu_4NF$ , THF; (3)  $K_2CO_3$ , MeOH; and (4)  $MsCl$ ,  $Et_3N$ ,  $CH_2Cl_2$ ) gave the desired hydroxy mesylate (**8**, mp 164–165 °C) in >85% overall yield. Anionic fragmentation then proceeded cleanly by deprotonation with sodium hydride (THF; 0 °C) to yield **9** (IR (Nujol) 1680, 1715  $cm^{-1}$ ; 80% yield).

With the relative stereochemistry in the two isolated rings now fixed, we began to add the required functionality at C-2, C-9, and C-12. The most crucial of the operations involved trans hydroxylation of the C-2–C-12 olefin in such a way that the newly added hydroxyl at C-2 would have the  $\alpha$  configuration as required for subsequent cyclization. While we anticipated that the bulk of the C-5  $\alpha$  substituent would direct both steps of an epoxidation–hydrolysis sequence to give the desired stereochemistry, the C-2–C-12 double bond of **9** was relatively unreactive with peracids<sup>8</sup> and it was necessary to deprotect C-4 temporarily prior to epoxidation. Thus debenzoylation ( $K_2CO_3$ , MeOH) preceded a hydroxyl-directed epoxidation (*t*-BuOOH,  $VO(acac)_2$ ,  $CH_2Cl_2$ ) and produced the  $\beta$ -oxide **10** (mp 103–104 °C) in 75% yield at 80% conversion. Acid-catalyzed glycol formation was somewhat sluggish but proceeded (2% aqueous  $H_2SO_4$ ,  $CH_3COCH_3$ ; 45 °C) to give the expected inversion at C-2 as shown in Scheme III by direct formation of the bridged tricyclic intermediate **11**<sup>9</sup> (mp 150–151 °C; 60% yield).

Final elaboration to trichodermol (**1**) was carried out straightforwardly. Thus methylation at C-9 (MeLi, THF; 80% yield), monobenzoylation at C-4 ( $PhCOCl$ ,  $C_5H_5N$ ; 0 °C; 86% yield) and oxidation at C-12 ( $CrO_3 \cdot 2C_5H_5N$ ,  $CH_2Cl_2$ ; 88% yield) gave **12** (mp 148–150 °C) which underwent regioselective dehydration ( $POCl_3$ ,  $C_5H_5N$ ; 60% yield) to give a 7:1 mixture of olefins. The major isomer **13** (mp 180–182 °C) was isolated by chromatography on silica gel and was converted into **1** as described previously for the corresponding acetate<sup>2</sup> ((1)  $Ph_3P=CH_2$ , THF; (2) MCPBA,  $CH_2Cl_2$ ). The racemic trichodermol thus produced (mp 123.5–125 °C (lit.<sup>2</sup> 124–125 °C)) was indistinguishable by TLC, IR, NMR, and MS from a sample of natural trichodermol kindly provided by Professor B. B. Jarvis of the University of Maryland.<sup>10</sup>

## References and Notes

- (1) S. Abrahamsson and B. Nilsson, *Proc. Chem. Soc.*, 188 (1964).
- (2) E. W. Colvin, S. Malchenko, R. A. Raphael, and J. S. Roberts, *J. Chem. Soc., Perkin Trans. 1*, 1989 (1973). See also S. C. Welch and R. Y. Wong, *Synth. Commun.*, **2**, 291 (1972); S. C. Welch and R. Y. Wong, *Tetrahedron Lett.*, 1853 (1972); D. J. Goldsmith, A. J. Lewis, and W. C. Still, *ibid.*, 4807 (1973); Y. Fugimoto, S. Yokura, T. Nakamura, T. Morikawa, and T. Tatsuno, *ibid.*, 2523 (1974); E. W. Colvin, S. Malchenko, R. A. Raphael and J. S. Roberts, *J. Chem. Soc., Perkin Trans. 1*, 658 (1978); B. B. Snider and S. G. Amin, *Synth. Commun.*, **8**, 117 (1978).
- (3) Y. Machida and S. Nozoe, *Tetrahedron*, **28**, 5113 (1972). In vitro model cyclizations: N. Masuoka, T. Kamikawa and T. Kubota, *Chem. Lett.*, 751 (1974); N. Masuoka and T. Kamikawa, *Tetrahedron Lett.*, 1691 (1976).
- (4) Dienol silyl ether **3** was prepared by silylation of the kinetic enolate of 4-methylcyclohex-3-en-1-one (a)  $LiNiPr_2$ , THF–HMPA; (b)  $t-BuMe_2SiCl$ ; cf. G. M. Rubottom and J. M. Gruber, *J. Org. Chem.*, **42**, 1015 (1977).
- (5) Cf. W. Herz, V. S. Iyer, and M. G. Nair, *J. Org. Chem.*, **40**, 3519 (1975).
- (6) We were unable to find more than traces of the other Favorskii product by a careful examination of the crude product and believe that the observed regioselectivity results from silyl oxygen-assisted  $\sigma$  overlap with the C-2 carbonyl.
- (7) J.-P. Pete, C. Portella, C. Monneret, J.-C. Florent, and Q. Khuong-Huu, *Synthesis*, 774 (1977).
- (8) Extended reaction of **9** with MCPBA gave competitive Baeyer–Villiger oxidation of the appended cyclohexenone.
- (9) The bridged structure **11** was distinguished from an analogous fused one (conceivably formed from the alternative C-2, C-12 glycol) by the NMR of the derived diacetate: NMR ( $CDCl_3$ )  $\delta$  3.70 (m, w/2 = 10 Hz, 1 H, H-11), 4.29 (dd,  $J = 2, 5$  Hz, 1 H, H-2), 5.30 (br d,  $J = 2$  Hz, 1 H, H-12), 5.41 (dd,  $J = 4, 8$  Hz, 1 H, H-4). Irradiation at  $\delta$  4.29 caused the tight doublet at 5.30 to collapse to a singlet.
- (10) This work was supported by NIH Grant 5 R01 CA23094.
- (11) Alfred P. Sloan Fellow, 1978–1980.

W. Clark Still,\*<sup>11</sup> Mei-Yuan Tsai

Department of Chemistry, Columbia University  
New York, New York, 10027

Received February 14, 1980

## Electronic Spectra of Model Oxy, Carboxy P450, and Carboxy Heme Complexes

Sir:

The optical spectra of the carboxy complex of reduced cytochrome P450 has been the subject of considerable experimental investigation.<sup>1–3</sup> In contrast to carboxyhemoglobin<sup>2</sup> and myoglobin,<sup>4</sup> the Soret band is split into two components with maxima at  $\lambda$  363 and 450 nm, the latter giving the name to this class of heme proteins which are mixed function oxidases. The spectroscopic behavior of the dioxygen complex of these enzymes, which is part of their normal enzymatic cycle, is more ambiguous. However, two studies<sup>5,6</sup> of the intact complex reveal a split Soret with broadened and blue-shifted components at  $\lambda$  340 and 420 nm. Model oxy<sup>7</sup> and carboxy<sup>8–10</sup> heme complexes with thiolate or mercaptide ligands appear to have very similar optical spectra to the intact proteins, with more uncertainty in the oxy complex.

To understand the origin of differences in their spectroscopic behavior, we have calculated the electronic spectra of model oxy and carboxy P450 complexes together with a model carboxy heme complex using a newly developed INDO method including transition metal complexes and extensive configuration interaction.<sup>11–13</sup> This program, with spectroscopic parameterization, has been used by us to successfully describe the ground state of model oxy and carboxy P450 complexes<sup>14</sup> and model oxy hemoglobin complexes,<sup>15</sup> accounting for the quadrupole splitting in Mössbauer resonance of these complexes. It has also been used to successfully describe the ground state and/or spectral properties of  $(FeCl_4)^-$ ,  $(CoCl_4)^{2-}$ ,  $(CuCl_4)^{2-}$ ,<sup>13</sup> and ferrocene.<sup>16</sup>

The geometry used for the six-coordinated ferrous P450 is based on an X-ray crystal structure of the porphyrin ring and the mercaptide ( $SCH_3^-$ ) and CO and  $O_2$  axial ligands in model compounds.<sup>17</sup> The same geometry was used for the model

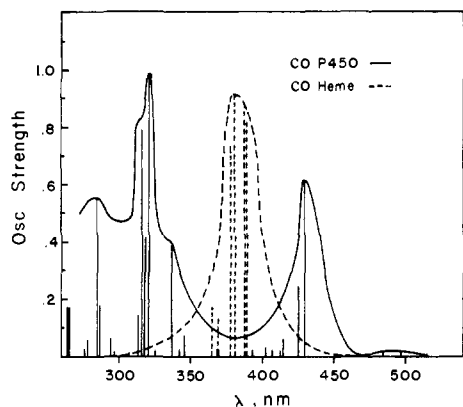


Figure 1. Calculated electronic transitions for model carboxy heme (---) and carboxy P450 complex (—).

carboxy heme compound but with an imidazole ligand replacing the mercaptide ligand.<sup>18</sup>

Figure 1 presents the calculated wavelength and oscillator strengths for electronic transitions in the model carboxy heme and carboxy P450 complexes. For convenience in comparison with experimental spectra, envelopes are drawn around the calculated oscillator strengths for each frequency and are not intended to reproduce the experimental band width. As shown in this figure, differences in the calculated spectra of these complexes are in striking agreement with their observed differences. The carboxy heme spectra has a single Soret peak composed of at least four major transitions centered around  $\lambda$  380 nm, exactly between the two components of the split Soret bands of the carboxy P450 spectra which have maxima at  $\lambda \approx 320$  and  $\approx 430$  nm. Again, as shown by the bars, each component of the split Soret is composed of many allowed transitions with significant oscillator strengths. Both complexes have several weak  $Q_0$  transitions around  $15\,000\text{ cm}^{-1}$ .

The origin of the differences in the Soret transitions between carboxy heme and carboxy P450 is clear from an analysis of the ground-state electronic structure of each complex and the way in which excited states mix by configuration interaction. In both carboxy heme and carboxy P450, the two highest occupied molecular orbitals are  $a_{2u}$  and  $a_{1u}$  porphyrin orbitals, respectively. The  $a_{2u}$  orbital has appreciable (15%)  $sp_z$  character in the P450 complex. The two lowest empty orbitals are the  $e_g\pi^*$ . It has been well established in earlier work<sup>19</sup> that the origin of both the  $Q_0$  and the Soret bands comes from configuration interaction between excited states involving these four orbitals. In the spectral calculations reported in Figure 1, not only these four states but a total of 132 singly and 50 doubly excited configurations were used for HbCO and 63 singly and 81 doubly excited states for P450 CO were used. These states were selected as the most important for each complex from many trial calculations systematically investigating single and double excitations. For neither complex were double excitations significant, accounting for <5% of the total configurations.

For both the carboxy Hb and carboxy P450 complexes,  $Q_0$  is pure  $a_{1u}, a_{2u} \rightarrow e_g\pi^*$  transition. For carboxy Hb, the many transitions composing the normal Soret band have about 50%  $a_{1u}, a_{2u} \rightarrow e_g\pi^*$  character and are substantially mixed with  $d_{x^2-y^2} \rightarrow e_g\pi^*$  and  $d_{xy} \rightarrow e_g\pi^*$  excitations. The three d orbitals involved in these excitations lie just below the  $a_{1u}$  and  $a_{2u}$  orbitals and none have any axial ligand character. The  $d_{x^2-y^2}$  orbital is totally localized on the iron while the two  $d_{xy}$  orbitals are  $\sim 40\%$  delocalized on porphyrin  $\pi$  orbitals. These interactions do not split the Soret and result in a "normal" Soret band.

In contrast to the carboxy heme complex, the four filled orbitals lying just below the  $a_{1u}$  and  $a_{2u}$  orbitals in the carboxy

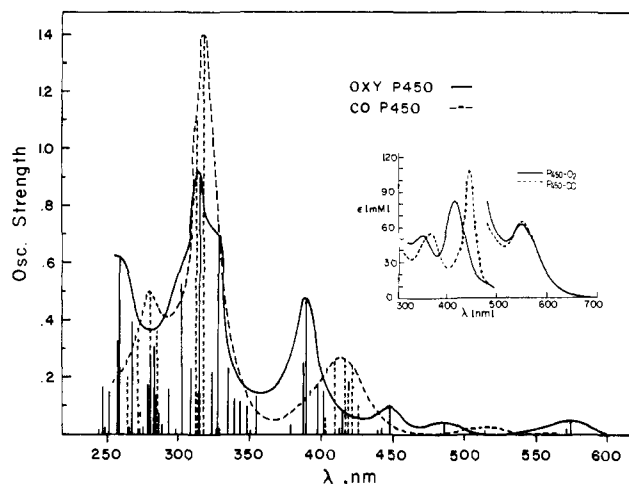


Figure 2. Calculated electronic transitions for model oxy P450 complex (—) and carboxy P450 complex (---).

P450 complex contain substantial sulfur as well as iron d character. Two of them are  $(S_x-S_y)-(d_{xz}-d_{yz})$  orbitals with 65 and 25% sulfur character, respectively. One is essentially a  $d_{xz}, d_{yz}$  orbital, with a small amount of sulfur character, and the fourth is 50%  $sp_z$ . The results of configuration interaction indicate that both components of the split Soret contain transitions, which are substantial mixtures of excitations from these four orbitals to  $e_g\pi^*$  with  $a_{1u}, a_{2u} \rightarrow e_g\pi^*$  excitations. It is this mixing which appears to cause the splitting and shifting of the Soret peak. As shown by the bar graphs, there are many such transitions which also include minor components such as  $d_{xy}$  and  $S_x-S_y \rightarrow b_{2u}\pi^*$  excitations.

Previous consideration of the origin of the split Soret using ground-state calculations obtained by the IEHT method also implicated  $S \rightarrow e_g\pi^*$  excitations mixing with  $a_{1u}, a_{2u} \rightarrow e_g\pi^*$  excitations as the origin of "hyper" spectra.<sup>2</sup> The quantitative spectral assignment presented here confirms this qualitative conclusion. Thus the origin of the split Soret appears to be due to the presence of high-energy occupied sulfur, d-containing orbitals which are absent in any heme protein with an imidazole axial ligand.

An implication of these results is that it is the sulfur ligand of cytochrome P450 which is responsible for the split Soret. The axial carboxy ligand is not involved substantially in the excitations which contribute to the Soret transitions. Thus, it might be expected that almost any reduced P450 ligand complex would have a split Soret. Indeed this has now been found to be the case for at least five other axial ligands: 1-phenylimidazole, dimethyl sulfide, thioxane, pyridene, and metyrapone complexed to reduced P450<sub>CAMP</sub>. It would appear that, in each case, the endogenous mercaptide ligand remains intact in these complexes.

As discussed, the behavior of the reduced oxy complex of P450 and model compounds is more controversial. Both normal and hyper spectra have been reported for model compounds and the intact protein.<sup>3,5,6</sup>

Figure 2 gives the results of our calculated spectra of a model oxy P450 complex, with the bars representing calculated transition energies and oscillator strengths. We see from this spectra that the oxy complex does indeed have a split Soret. In agreement with most recent experimental results for the protein,<sup>5</sup> it also seems broadened and shifted slightly to higher energy compared to the carboxy P450 complex.

The origin of the split Soret transition in oxy P450 is the same as in the carboxy complex. The ground state of the oxy P450 complex also has four sulfur-containing orbitals just below the highest occupied  $a_{2u}$  and  $a_{1u}$  orbitals. Again, it is mixing of excitation from all six of these orbitals to  $e_g\pi^*$  that

accounts for the split Soret. However, the O<sub>2</sub> complex differs from the CO complex in two ways. The filled orbitals which have sulfur character also have oxygen character. In addition, the lowest empty orbital is an Oπ\* orbital, absent in the carboxy complex, followed by the two e<sub>g</sub>π\* orbitals. Excitations from a<sub>1u</sub> and a<sub>2u</sub> to Oπ\* as well as to e<sub>g</sub>π\* play a role in both components of the Soret band. This additional mixing leads to many more allowed transitions in the Soret region, causing the broadening and blue shift to λ 420 nm which has made the oxy P450 complex less easy to characterize. Such behavior should occur for reduced P450 whenever it has a second axial ligand which can interact with the porphyrin and iron π systems and the sulfur ligand. Work is continuing to determine the effect of variation in ligand geometry on these spectra.

**Acknowledgment.** We thank Dr. David Dolphin for making this unpublished data on oxy P450 available to us. We also thank Dr. Peter Debrunner for many helpful discussions and Visiting Scientist Dr. Amiram Goldblum for his interest and help in preparation of this manuscript. We also are grateful to Dr. Michael Zerner for his continued guidance in the use of his INDO program. We gratefully acknowledge support for this work from NIH Grant No. GM 27943 and from a National Resource for Computations in Chemistry (NRCC) computation award.

### References and Notes

- (1) Hanson, L. K.; Eaton, W. A.; Sligar, S. G.; Gunsalus, I. C.; Gouterman, M.; Connell, C. R. *J. Am. Chem. Soc.* **1976**, *98*, 2572.
- (2) Hanson, L. K.; Sligar, S. G.; Gunsalus, I. C. *Croat. Chem. Acta* **1977**, *49*, No. 2, 237-250.
- (3) Ullrich, V.; Ruf, H. H.; Wende, P. *Croat. Chem. Acta* **1977**, *49*, No. 2, 213-222.
- (4) Churg, A. K.; Makinen, M. W. *J. Chem. Phys.* **1978**, *68*, No. 4, 1913-1925.
- (5) Peterson, J. A.; Ishimura, Y.; Griffin, B. W. *Arch. Biochem. Biophys.* **1972**, *149*, 197-208.
- (6) D. Dolphin, private communication.
- (7) Chang, A. K.; Dolphin, D. *J. Am. Chem. Soc.* **1976**, *98*, 1607.
- (8) Collman, J. P.; Sorrell, T. N. *J. Am. Chem. Soc.* **1975**, *97*, 4133-4134.
- (9) Chang, A. K.; Dolphin, D. *Proc. Natl. Acad. Sci. U.S.A.* **1976**, *73*, No. 10, 3338-3342.
- (10) Stern, J. O.; Peisach, J. *J. Biol. Chem.* **1974**, *249*, No. 23, 7495-7498.
- (11) Ridley, J.; Zerner, M. *Theor. Chim. Acta* **1973**, *32*, 111.
- (12) Ridley, J.; Zerner, M. *Theor. Chim. Acta* **1976**, *42*, 273.
- (13) Bacon, A. D.; Zerner, M. C. *Theor. Chim. Acta* **1979**, *53*, 21.
- (14) Rohmer, M. M.; Loew, G. H., *Int. J. Quantum Chem.*, in press.
- (15) Herman, Z. S.; Loew, G. H. *J. Am. Chem. Soc.* **1980**, *102*, 1815.
- (16) Zerner, M.; Loew, G. H.; Kirchner, R. F.; Mueller-Westerhoff, U. T. *J. Am. Chem. Soc.* **1980**, *102*, 589.
- (17) Tang, S. C.; Koch, S.; Papaefthymiou, G. C.; Foner, S.; Frankel, R. B.; Ibers, J. A.; Holm, R. H. *J. Am. Chem. Soc.* **1976**, *98*, 2414-2434.
- (18) Collman, J. P.; Gagne, R. R.; Reed, C. A.; Robinson, W. T.; Rodley, G. A. *Proc. Natl. Acad. Sci. U.S.A.* **1974**, *71*, 1326.
- (19) Gouterman, M. In "The Porphyrins", D. Dolphin, Ed.; Academic Press: New York, 1977, Vol. III, p. 1.

Gilda H. Loew\*

Life Sciences Division, SRI International  
Menlo Park, California 94025

Marie-Madeleine Rohmer

Quantum Chemistry Laboratory, University Louis Pasteur  
Strasbourg F67000, France

Received October 5, 1979

### Electronic Spectrum of Model Cytochrome P450 Complex with Postulated Carbene Metabolite of Halothane

Sir:

The widely used anesthetic halothane (2-bromo-2-chloro-1,1,1-trifluoroethane) undergoes oxidative metabolism by the cytochrome P450s in the presence of molecular oxygen and 2 reducing equiv of NADPH. While it was once believed that intermediate metabolic products from this oxidative metabolism in the pathway to forming trifluoroacetic acid<sup>1</sup> were re-

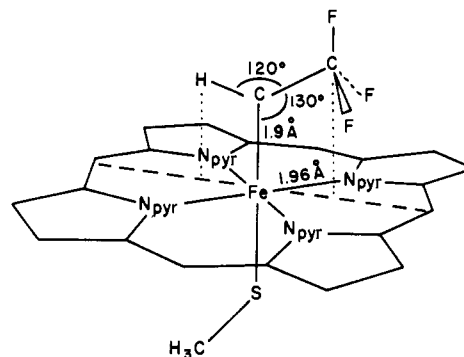


**Figure 1.** Model CF<sub>3</sub>CH carbene P450 complex. Porphyrin and mercaptide ligand geometry was taken from model X-ray studies.<sup>18</sup> Carbene bond angles and torsion angles were chosen to minimize steric hindrance of CF<sub>3</sub> group with porphyrin ring with optimized C-Fe distance.

sponsible for observed renal and hepatic toxicity in man, there is now convincing evidence<sup>2-4</sup> that products of anaerobic reductive metabolism also catalyzed by cytochrome P450s<sup>2,3</sup> are the toxic substances. It is particularly interesting that, under anaerobic conditions (O<sub>2</sub> < 50 μM), reduced cytochrome P450 in liver microsomal suspension forms a complex with halothane which exhibits an unusual Soret band at 470 nm. Such a spectrum has also been found in complexes of halothane with a reconstituted spherical phospholipid system containing rat or human cytochrome P450, reductase and NADPH.<sup>5</sup> This spectrum has been attributed to a ferrous cytochrome P450 complex in which a trifluoromethyl carbene (CF<sub>3</sub>CH), formed by two-electron reductive elimination of chloride and bromide from the halothane molecule,<sup>6</sup> binds directly to the iron as an axial ligand.

The most compelling evidence for the formation of such a carbene complex with ferrous cytochrome P450 is that an identical spectra is obtained in the presence of 2,2,2-trifluorodiazethane. This species readily undergoes a metal-catalyzed decomposition to dinitrogen and the CF<sub>3</sub>CH carbene.<sup>6</sup>

In both microsomal suspension<sup>5,7,8</sup> and reconstituted systems,<sup>5</sup> only difference spectra between the complex formed by addition of excess halothane and other complexes are obtained. For example, in the difference spectra between the carboxy and halothane complexes, the λ 450 nm band disappears and the λ 470 nm band appears. This is the only transition whose appearance is clearly demonstrated in observed spectra. It is not possible with membrane-bound cytochrome P450 to determine if there is another absorption band which corresponds to a second component of the Soret transition. In soluble carboxy P450<sub>CAMP</sub>, this second band is found at ~363 nm, a region of intense protein absorption in both the reconstituted and microsomal systems of the carbene complex. Thus the question whether the postulated carbene complex, like the carboxy complex, has a split Soret spectrum is unresolved.

In the work reported here we have calculated the electronic spectrum of a model ferrous cytochrome P450-trifluoromethylcarbene complex, to further explore the hypothesis that a carbene complex of ferrous cytochrome P450 is responsible for the observed red-shifted Soret transition upon halothane addition, and to more fully characterize the spectrum of such a complex.

In this study, we have used a newly developed INDO method which includes transition metal complexes and extensive configuration interaction.<sup>9-11</sup> It has been used by us to successfully describe the ground-state and electronic spectra of oxy and carboxy P450,<sup>12,13</sup> oxy and carboxy heme complexes,<sup>14-16</sup> and ferrocene.<sup>17</sup>

The model carbene P450 complex used in this study is shown in Figure 1. The geometry of the porphyrin ring and methyl-